



Cite this: *Environ. Sci.: Nano*, 2020, 7, 2073

## Biological effects of allergen–nanoparticle conjugates: uptake and immune effects determined on hAELVi cells under submerged vs. air–liquid interface conditions†

Robert Mills-Goodlet, <sup>a</sup> Milena Schenck, <sup>b</sup> Aline Chary, <sup>c</sup> Mark Geppert, <sup>a</sup> Tommaso Serchi, <sup>c</sup> Sabine Hofer, <sup>a</sup> Nobert Hofstätter, <sup>a</sup> Andrea Feinle, <sup>b</sup> Nicola Hüsing, <sup>b</sup> Arno C. Gutleb, <sup>c</sup> Martin Himly <sup>a</sup> and Albert Duschl <sup>a\*</sup>

Type I hypersensitivity reactions against environmental entities, *i.e.* allergens, are an ever growing problem, with increasing numbers of affected individuals in Western countries. In parallel, nanotechnology has been growing during the past decades, entering more and more areas of application in everyday life. Exposure to allergens may occur in a combined way with environmental particulate matter or (nano-)particles potentially abundant at the workplace. Such combinations may thus affect workers and consumers alike. The present study conceived a methodological and mechanistic approach based on recombinant allergen–SiO<sub>2</sub> nanoparticle conjugates and the novel hAELVi cell line as two well-defined model systems to investigate the effects of co-exposure towards allergens and nanoparticles. We applied pristine nanoparticles, allergen–nanoparticle conjugates and unbound allergen under submerged and air–liquid interface conditions. The uptake kinetics and mechanisms, cellular localization and resulting immune responses were studied in hAELVi cells, a cell line derived from human alveolar epithelium showing the characteristics of type I epithelial cells. Modification in the uptake kinetics as well as an increase in pro-inflammatory cyto-/chemokine expression was observed under submerged conditions, but much less under air–liquid interface conditions. While for mechanistic investigations the submerged culture system still proved suitable, more robust and cost-effective, these culture conditions showed considerable deviations in cellular susceptibility observed under more realistic conditions.

Received 27th November 2019,  
Accepted 5th May 2020

DOI: 10.1039/c9en01353a

rsc.li/es-nano



### Environmental significance

SiO<sub>2</sub> nanoparticles are among the most produced and widely used nanoparticles, leading to a high degree of environmental exposure. The release into the environment can facilitate interactions with airborne allergens which are omnipresent. These interactions can modify the biological effect of the allergen upon inhalation. Determination of such alterations upon inhalation may be relevant for individuals suffering from allergic disease. The present study demonstrates that conjugate formation of allergens and nanoparticles modifies the uptake kinetics and mechanisms, which furthermore impacts the biological response observed in alveolar epithelial cells.

## 1 Introduction

Allergy is an adverse reaction of the immune system against stimuli tolerated by most people. During the past 50 years,

allergic diseases have significantly increased in prevalence.<sup>1,2</sup> By now, more than 150 million people are suffering from allergic diseases in Europe<sup>3</sup> and more than a billion individuals on a worldwide scale.<sup>4</sup> Environmental allergen sources include pollen, animal saliva, insect venom and food. Allergenic foods include nuts, eggs, shellfish and fish, affecting about 6% of adults.<sup>5</sup> Occupational respiratory disease has been described for the seafood industry, where 2–36% of workers suffer from allergic asthma due to regular inhalation of seafood-derived wet aerosols or allergen-loaded dusts resulting from surface treatment with wet jets or compressed air.<sup>6</sup> Altogether, respiratory allergies show the highest prevalence with around 235 million people suffering

<sup>a</sup> Department of Biosciences, Paris Lodron University of Salzburg, Hellbrunnerstrasse 34, Salzburg 5020, Austria. E-mail: albert.duschl@sbg.ac.at; Tel: +43 662 8044 5731

<sup>b</sup> Department of Chemistry and Physics of Materials, University of Salzburg, Salzburg 5020, Austria

<sup>c</sup> Luxembourg Institute of Science and Technology (LIST), Environmental Research and Innovation (ERIN) Department, Belvaux, Grand Duchy of Luxembourg

† Electronic supplementary information (ESI) available. See DOI: 10.1039/c9en01353a

from allergic asthma.<sup>7–9</sup> Moreover, due to climate change, the exposure durations for seasonal allergens, like tree, grass and weed pollen, seem to be increasing.<sup>10</sup> Consequently, airborne allergens represent major causes for pulmonary diseases.<sup>11</sup> Concerning allergic sensitization, the dominant tree pollen found in Central and Northern Europe is from birch and other members of the *Betulaceae* family.<sup>12</sup> Their high abundance leads to a high seasonal exposure to birch pollen and to its major allergen Bet v 1, which is readily available as a highly purified and well-characterized recombinant protein.

Production and use of engineered nanoparticles (NPs) have increased significantly during the past decades. The estimated production volume of NPs ranges from 60 000 tons per year<sup>13</sup> to 11.5 million tons per year<sup>14</sup> worldwide for the ten most produced NPs (TiO<sub>2</sub>, ZnO, SiO<sub>2</sub>, FeO<sub>x</sub>, AlO<sub>x</sub>, CeO<sub>x</sub>, carbon nanotubes (CNTs), fullerenes, Ag and quantum dots). Out of these ten materials, SiO<sub>2</sub> NPs are among the most produced particles by weight with an estimated 5500 tons per year<sup>15</sup> to 1.5 million tons per year.<sup>14</sup> The applications for SiO<sub>2</sub> NPs include consumer products, cosmetics, food additives, tyres, agriculture and medicine,<sup>16–23</sup> leading to a higher exposure in the environment. The biological impact of crystalline silica (0.5–10 µm) has been associated with silicosis, lung cancer, pulmonary tuberculosis and emphysema.<sup>24</sup> In general, smaller amorphous SiO<sub>2</sub> NPs are considered less toxic compared to their larger crystalline counterparts. Studies in recent years have shown that SiO<sub>2</sub> NPs can induce oxidative stress and cytotoxicity depending on the tested material and cellular model.<sup>25,26</sup> Due to the wide use of SiO<sub>2</sub> NPs in industry and in consumer products, human exposure extends from occupational settings to everyday life. The major entry portal into the body at the workplace is *via* inhalation. Due to their small size, aerosolized NPs can reach and deposit in the deepest parts of the lung, the alveoli.<sup>27,28</sup> Aerosolized particles may represent a vivid interaction partner for airborne allergen sources, such as pollen fragments of trees, grass and weeds. Due to the NPs' high surface energy and resulting activity to form a protein corona,<sup>29</sup> allergenic proteins will coat NPs as soon as they come into contact with the particle surface. It has been shown previously that such interactions between gold NPs and allergenic molecules can have an impact on the allergic response of basophils derived from patients.<sup>30</sup> The authors showed that basophil activation was modulated in basophils from individual patients, when the allergens used were bound to NPs, compared to the same amount of free allergen. Moreover, an increased protease activity could be measured for the dust mite allergen Der p 1 when it was bound to NPs. These results indicate that the binding to NPs might influence the protein structure and epitope accessibility. A substantial donor variability may be explained by recognition of different epitopes by the donors.

As inhalation is the major entry route for both allergens and NPs, we wanted to investigate the effect of co-exposure *via* inhalation. The alveolar epithelium is composed of two different cell types, the alveolar epithelial type I cells, which

cover the majority of the surface and permit gas exchange, and the alveolar epithelial type II cells, which can differentiate into type I cells.<sup>31</sup> The inside of the alveoli is covered by a thin layer of alveolar surfactant, which is produced by type II epithelial cells. Primary human alveolar epithelial cells are not available for the type of study performed here, so researchers rely on stable cell lines. Nearly all *in vitro* studies investigating the impact of NPs on the alveolar barrier have been performed using the adenocarcinomic human alveolar basal epithelial cell line A549, which was isolated from cancerous lung tissue from a 58-year-old male<sup>32</sup> A549 cells resemble alveolar type II cells,<sup>33</sup> while up to 95% of the alveolar surface is covered in alveolar type I cells. The recently established human alveolar epithelial cell line called human alveolar epithelial lentiviral immortalized (hAELVi) cells was isolated from healthy lung tissue and immortalized using a lentiviral vector.<sup>34</sup> This cell line shows characteristics of alveolar type I cells including but not limited to the expression of ZO-1, the formation of intercellular tight junctions and the expression of caveolin-1.<sup>34</sup> The hAELVi cells are currently considered as a highly interesting new model that allows for better mimicking of the bulk of the alveolar epithelial surface.

For modelling realistic situations in the human lung, submerged cell culture conditions are not ideal since, *in vivo*, alveolar cells are separated from the gas phase by a thin layer of lung lining fluid, which contains a mix of phospholipids and the surfactant proteins A–D. The advantages of a submerged culture are ease of handling, lower price and better suitability for high-throughput formats; for this reason, this type of model still has its uses. However, studying cell exposure at the air–liquid interface (ALI) closer mimics the *in vivo* situation. Under ALI conditions, cells are grown on Transwell inserts, receiving nutrients only from the basolateral side. So far, very few studies have been conducted using hAELVi cells cultured at the ALI.<sup>34,35</sup> The exposure of ALI-cultured cells with NPs requires special equipment, such as the ALICE-Cloud system where NPs are aerosolized from the liquid state and tiny droplets are deposited onto the confluent lung epithelial cell layer. Due to the thin liquid layer on top of the cells under ALI conditions, there are fewer problems with NP agglomeration, diffusion, sedimentation, dissolution, *etc.*, compared to a submerged culture where the resulting differences between the administered dose and the dose delivered to the cell surface have to be taken into account.<sup>36–38</sup>

The present study was not designed to investigate risk to humans, as it does not reflect an actual human exposure situation, which may be addressed in follow-up studies. The purpose of this methodological and mechanistic study was to investigate the interactions of allergens and nanoparticles and their consequences for initiation events or potential adverse outcome pathways upon inhalation. We therefore established a well-defined allergen-doped particulate model system. The working hypothesis for the present study was that non-covalent conjugation, *i.e.* surface attachment, of allergen to nanoparticle impacts the uptake of the respective allergen



and the biological consequences inside the cells. Possible mechanisms could be an increased delivery of the allergen to the cells or the involvement of different uptake pathways. In addition, the accessibility of allergen epitopes could be changed due to non-random binding of the protein to the NP surface or to changes in protein structure. The observation that binding of a protease to gold NPs substantially increased its enzyme activity supports this hypothesis.<sup>39</sup> The aforementioned model system consisted of the recombinant birch pollen allergen Bet v 1 and SiO<sub>2</sub> NPs, which are generally considered as biologically inert. Recombinant Bet v 1 was used as a very well-characterized allergen allowing specific labelling strategies. To employ the most reliable and realistic conditions we chose a strategic approach where hAELVi cells were (i) cultured under submerged conditions for broader profiling experiments followed by (ii) more specific readouts when hAELVi cells were cultured at the ALI. The biological effects investigated included time-resolved uptake of unbound *vs.* particle-bound allergen into the cells, determination of the mechanisms involved in cell uptake, and potential initiation of an immune response as monitored by cyto-/chemokine expression profiling. Of note, inhaled allergens arrive mainly bound to carriers like dander or pollen fragments under real-life conditions.<sup>40–42</sup>

## 2 Materials and methods

### 2.1 SiO<sub>2</sub> nanoparticle synthesis and characterization

Mesoporous silica nanoparticles were prepared as previously described.<sup>43</sup> A detailed description is included in the ESI.† For the quantification of the Si content of SiO<sub>2</sub> NPs in aqueous and cell culture suspensions, the blue silicomolybdic assay was used as previously described<sup>44</sup> with a minor adaptation for microtiter plates. For further details, see the ESI.† The size distribution of the SiO<sub>2</sub> NPs in the cell culture medium was determined by nanoparticle tracking analysis (NTA). For NTA measurements, the samples were diluted in pure water to a final concentration of 1 µg mL<sup>-1</sup> and the size was measured using a NanoSight LM10 instrument (Malvern, Malvern, UK) by capturing 10 videos of 20 seconds length per measurement. Every measurement series was repeated 3 times. For primary particle size determination, scanning electron microscopy (SEM) was conducted upon drying, light manual grinding (to break up large agglomerates) and mounting onto a conductive double-sided carbon tape. The measurement was performed on a Zeiss ULTRA Plus SEM operated at 2 kV accelerating voltage using an in-lens detector.

### 2.2 Stability of the NP suspension and determination of delivered dose

A detailed description of the NP suspension stability testing is provided in the ESI.† Determination of the delivered NP dose under submerged culture conditions was performed by applying the *in vitro* sedimentation deposition dosimetry (ISDD) model.<sup>45</sup> Size distribution data obtained by NTA were used (for a description of the method, see above), and the

Harvard volumetric centrifugation method<sup>46</sup> was applied in order to determine the effective mesoporous particle and agglomerate density required as input parameters for ISDD.

### 2.3 Protein expression/purification, labelling and SiO<sub>2</sub> NP conjugate formation

Recombinant Bet v 1 was produced and purified according to previously published protocols.<sup>47–49</sup> Fluorescence labelling of Bet v 1 using pHrodo or FITC was performed as described.<sup>49</sup> For the uptake quantification with flow cytometry pHrodo was used, and for the microscopic quantification FITC was used. A detailed description of the labelling procedure can be found in the ESI.† Coupling of Bet v 1 to SiO<sub>2</sub> NPs was performed as described by Grotz *et al.* (2018).<sup>49</sup> For a detailed description, see the ESI.† Five µg mL<sup>-1</sup> Bet v 1 were bound to 50 µg mL<sup>-1</sup> SiO<sub>2</sub> NPs to avoid the presence of unbound Bet v 1 in the supernatant.

### 2.4 Cell culture

Human alveolar epithelial lentivirus immortalized (hAELVi) cells were obtained from InSCREENeX (Braunschweig, Germany). For routine culture, cells were kept in 75 cm<sup>2</sup> flasks, coated with huAEC coating solution, in cell culture medium (CCM: 99% huAEC medium supplemented with 1% penicillin/streptomycin) at 37 °C and 5% CO<sub>2</sub>. Cells were sub-cultured every 3–4 days according to the protocol described in the documentation provided by the cell distributor. For the experimental incubation, 1.5 × 10<sup>5</sup> cells were seeded in 500 µl CCM per well in a 24-well plate and grown for 48 h. Cells of passage numbers between 24 and 46 were used for the experiments. For confocal microscopy, submerged and ALI-cultured cells were seeded onto transparent 24-well ThinCert™ cell culture inserts (Greiner, Kremsmünster, Austria) with a pore diameter of 0.4 µm at a density of 5 × 10<sup>4</sup> cells and grown for 14 days with regular medium changes every 2–3 days. For incubations under ALI conditions, 5 × 10<sup>4</sup> cells were seeded on Transwell inserts with 200 µl CCM on the apical and 800 µl CCM on the basolateral side. Proper cell growth and formation of a functional epithelial barrier was monitored by regular measurements of the transepithelial electrical resistance (TEER) as previously described,<sup>34</sup> resulting in TEER values of 1500–2000 Ω cm<sup>2</sup> within three weeks (Fig. S1†). After reaching TEER values of >1500 Ω cm<sup>2</sup>, the cells were transferred to ALI conditions by removing the medium from both apical and basolateral sides and adding 450 µl of CCM on the basolateral side. The presence of pulmonary surfactant was determined *via* the DMP/O droplet test, described in detail in the ESI.†<sup>50</sup>

### 2.5 Exposure conditions

For the exposure, the cells were taken out of the incubator, the medium was aspirated and the cells were incubated in cell culture medium containing either Bet v 1 only, SiO<sub>2</sub> NPs only or Bet v 1/SiO<sub>2</sub> NP conjugates. For experiments analysed



by flow cytometry, Bet v 1 was covalently labelled with pHrodo; for experiments analysed by confocal laser scanning microscopy, Bet v 1 was covalently labelled with FITC. After the desired incubation time, the media were collected, and the cells were washed twice with 1 mL PBS before further investigation. For the inhibition study, the cells were pre-incubated with CCM containing endocytosis inhibitors (Table S2†) for 30 to 90 min, depending on the inhibitor. For ALI exposure, the cells remained under ALI conditions, as described above, for at least 24 h before exposure was started. Cells were transferred to the metal base of a Vitrocell® Cloud-24 system (Vitrocell®, Waldkirch, Germany) pre-heated to 37 °C. Afterwards, the cells were exposed, with either unbound or NP-bound Bet v 1 at a concentration of 4.44  $\mu\text{g cm}^{-2}$  in 0.5× PBS, for 20 min using an Aeroneb Pro® (Aerogen, Ratingen, Germany) vibrating membrane nebulizer in conjunction with the Vitrocell® Cloud-24 system. After 20 min, the majority of the nebulized compound had settled onto the cells with a deposition efficiency of 50–80%.<sup>51</sup>

## 2.6 Cell viability

To determine the cell viability, both the neutral red (NR)<sup>52</sup> and the CellTiterBlue® (CTB)<sup>53</sup> assays were used. The CTB and NR assays were performed according to the manufacturer's instructions. Further details are described in the ESI.† Cell viability was calculated as percentage viability compared to control cells (treated with CCM only).

## 2.7 Flow cytometry

For flow cytometry analysis, cells were seeded in 24-well plates for submerged exposure or in 24-well Transwell inserts for ALI exposure. After exposure, cells were trypsinized with 100  $\mu\text{l}$  of trypsin-EDTA solution for 5 min at 37 °C. After washing, the cells were resolved in 400  $\mu\text{l}$  of PBS containing 3 mM EDTA and analysed using a FACS Canto II or an LSRIFortessa (BD Biosciences, San Jose, USA) analyzer. Uptake of pHrodo-labelled protein was determined by measuring the median fluorescence intensity (MFI) of the treated and untreated cells.

## 2.8 Confocal microscopy

For a qualitative assessment of NP uptake and presence of surfactant proteins A, B and C, confocal laser scanning microscopy (CLSM) with Airyscan was applied using an LSM 880 microscope (Carl Zeiss Microscopy GmbH, Jena, Germany), as described in detail in the ESI.†

## 2.9 Cytokine expression analysis

The quantification of cytokine expression was performed using quantitative real-time PCR as described in the ESI.†

## 2.10 Statistical evaluation

The results represent the mean values and standard deviations (SDs) of three experiments performed individually. Different individually prepared passages of cells were used for cell culture experiments. The unpaired *t*-test was used to

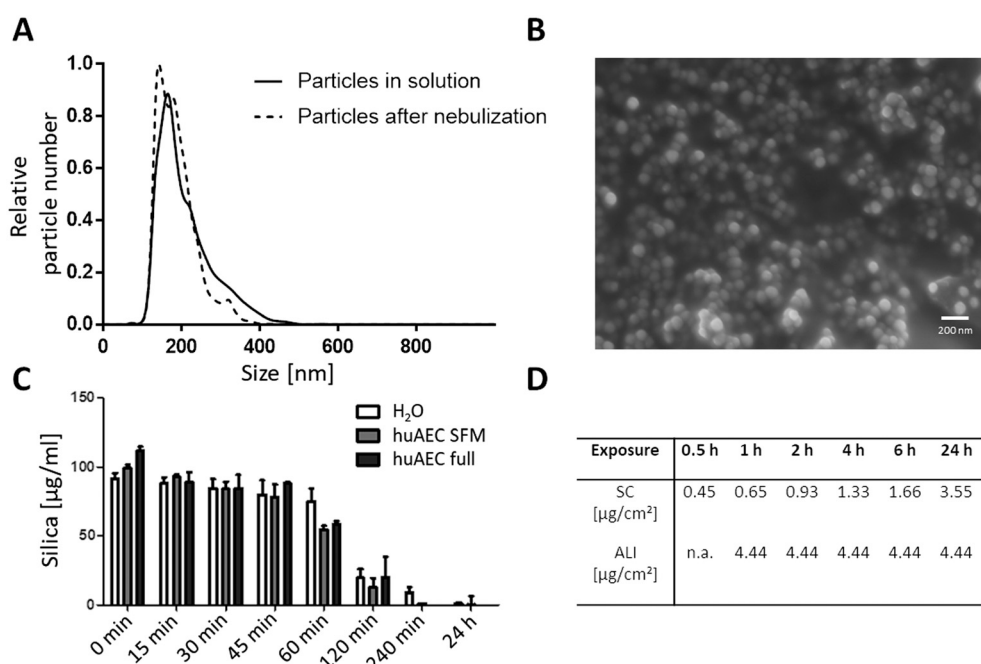


**Fig. 1** Characterization of SiO<sub>2</sub> NPs. (A) Size determination in media using NTA. (B) Size determination of primary particles using SEM. (C) Suspension stability of NPs in different media over time. Silica content measured using the blue silicomolybdic assay. H<sub>2</sub>O: particles incubated in milliQ water, huAEC SFM: particles incubated in huAEC medium without serum, huAEC full: particles incubated in huAEC medium containing serum. (D) Delivered dose estimated by ISDD for submerged conditions (SC) and ALI for specific exposure times.



analyse two sets of data, while ANOVA followed by a Bonferroni *post hoc* test was used for analysis between groups. A  $p > 0.05$  was considered as not statistically significant.

### 3 Results

#### 3.1 Characterization of $\text{SiO}_2$ NPs and formation of allergen-NP conjugates

Particle size analysis resulted in a distribution of the mesoporous  $\text{SiO}_2$  NPs with an average diameter of  $203 \pm 4$  nm in the CCM, as calculated from three individual measurements using NTA (Fig. 1A). A primary particle size of  $73 \pm 11$  nm was determined by analysing SEM pictures (Fig. 1B) which was done by measuring 100 particles using Fiji software.<sup>54</sup> The suspension stability towards sedimentation of the  $\text{SiO}_2$  NPs was similar in the different media, as the measured silica content of the sedimentation samples remained constant for up to 60 min in  $\text{H}_2\text{O}$ , serum-free and serum-containing hUAEC medium measured using the blue silicomolybdic assay.<sup>44</sup> At incubation times of 2 hours and longer, the measured silica content decreased rapidly (Fig. 1C); coinciding with the ISDD modelling data

showing a gradual increase of NPs at the surface of the adherent cells (Fig. 1D). For the deposited dose under submerged conditions the ISDD calculations yielded NP concentrations of 0.45 to  $3.55 \mu\text{g cm}^{-2}$  for the different exposure time points. The deposition efficiency of the Vitrocell Cloud system has been estimated to be between 50% and 80%, leading to a deposited dose of NPs onto the cells of between 2.22 to  $3.55 \mu\text{g cm}^{-2}$ .<sup>51</sup> For both the  $\text{SiO}_2$  NPs and purified Bet v 1 the endotoxin contamination was determined using the HEK-Blue TLR4 assay (Invivogen, San Diego, USA). For the used concentrations of particles, the LPS amount was below the detection limit of the assay; which is  $0.02 \text{ ng mL}^{-1}$ . The LPS amount of the recombinant Bet v 1 was also below the detection limit of the assay for the protein concentration used for cell exposure.

#### 3.2 Impact of NPs, allergen and conjugates on cell viability

Incubating hAELVi cells growing under submerged culture conditions with  $\text{SiO}_2$  NPs in concentrations ranging from 25 to  $400 \mu\text{g mL}^{-1}$  did not significantly affect the viability, measured by both CTB and neutral red assays. We used

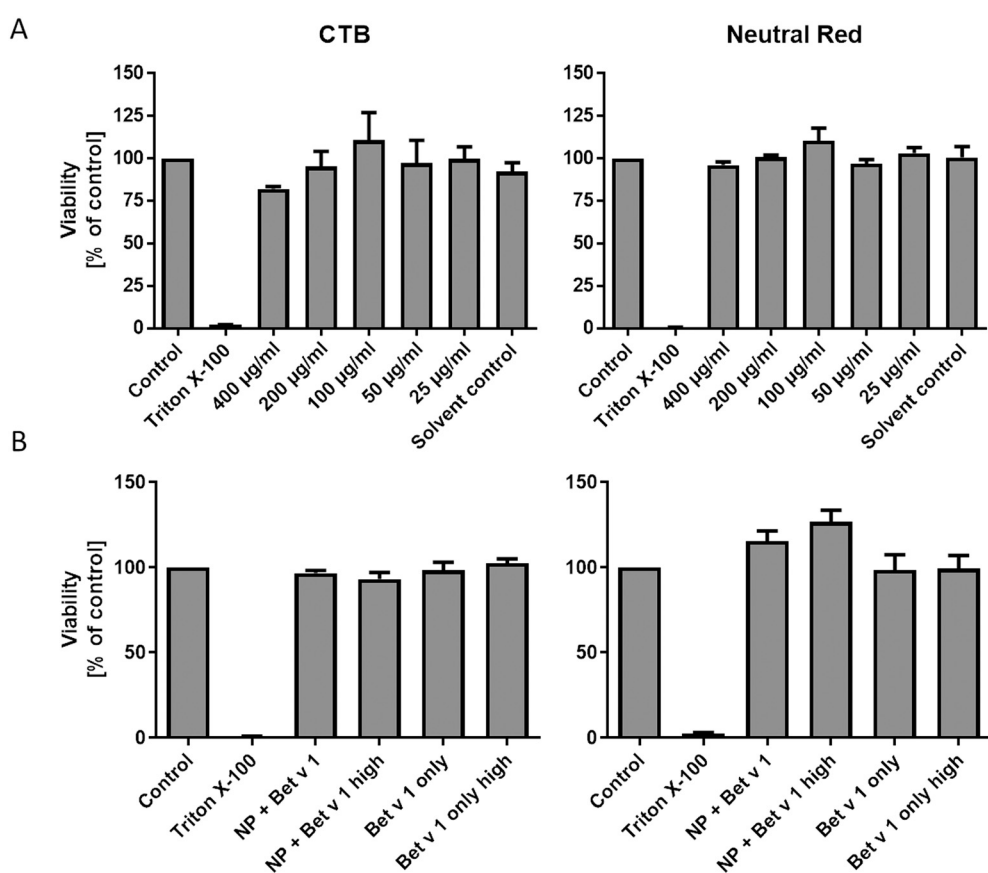


**Fig. 2** Viability of hAELVi cells incubated with  $\text{SiO}_2$  NP concentrations from  $400$  to  $25 \mu\text{g mL}^{-1}$  (A) and after incubation with unbound Bet v 1 and Bet v 1-NP conjugates (B). Control: cells incubated in CCM only. Triton X-100: cells incubated in CCM with 1% Triton X100,  $400$ – $25 \mu\text{g mL}^{-1}$ : cells incubated in CCM with respective amounts of NPs, solvent control: cells incubated in CCM with NP solvent. NP + Bet v 1: cells incubated with  $50 \mu\text{g mL}^{-1}$  NPs together with  $5 \mu\text{g mL}^{-1}$  Bet v 1, NP + Bet v 1 high: cells incubated with  $500 \mu\text{g mL}^{-1}$  NPs together with  $50 \mu\text{g mL}^{-1}$  Bet v 1, Bet v 1 only: cells incubated with  $5 \mu\text{g mL}^{-1}$  Bet v 1, Bet v 1 only high: cells incubated with  $50 \mu\text{g mL}^{-1}$  Bet v 1. Statistical analysis was performed using ANOVA with Bonferroni *post hoc* test.



concentrations of 25 to 400  $\mu\text{g mL}^{-1}$ , which is far higher than any realistic human inhalation exposure, since we wanted to cover a wide dose range to study the principal mechanisms of allergen/NP effects on hAELVi cells. However, even at the highest dose, no significant decrease in cell viability could be measured, demonstrating the lack of toxicity of the NPs used under our conditions. Similarly, the viability of the hAELVi cells was not affected by incubation with the allergen-NP conjugates or the allergen alone (Fig. 2). By visual inspection, similar confluence and morphology of hAELVi cells cultured under submerged *vs.* ALI conditions were observed (Fig. 5).

### 3.3 hAELVi cells express pulmonary surfactant under ALI conditions

hAELVi cells cultured at the ALI showed growth parameters regarding formation of a functional epithelial barrier as previously described.<sup>34</sup> A difference of the hAELVi cell growth behaviour under ALI *vs.* submerged culture conditions was

observed regarding secretion of surfactant using the DMP/O droplet test. For the cells cultured under submerged conditions no droplet is formed and the added DMP/O collects around the edge of the well (Fig. 3A), while a stable droplet of DMP/O can be seen on the cells cultured under ALI conditions (Fig. 3B). To determine the presence of surfactant proteins, antibodies for surfactant protein A-C were used. All three antibodies showed a green fluorescent signal in the hAELVi cells (Fig. 3D-F), while in the secondary antibody control no fluorescent signal can be seen (Fig. 3C). Out of the three different tested surfactant proteins the most pronounced green fluorescence was observed for surfactant protein C with an even distribution of the signal across the cytosol. For surfactant protein A the signal was also distributed across the cytosol but with lower intensity than for surfactant protein C. The signal for surfactant protein B is the least pronounced of the three.

### 3.4 Time-resolved uptake of free *vs.* $\text{SiO}_2$ NP-bound Bet v 1

To investigate the uptake kinetics of free and  $\text{SiO}_2$  NP-bound Bet v 1, hAELVi cells were incubated for 30 min, 1, 2, 4, 6 and 24 h with 5  $\mu\text{g mL}^{-1}$  Bet v 1 alone or with 5  $\mu\text{g mL}^{-1}$  Bet v 1 coupled to 50  $\mu\text{g mL}^{-1}$   $\text{SiO}_2$  NPs. hAELVi cells accumulated both free and NP-coupled Bet v 1 under submerged conditions, as indicated by the increase in cellular fluorescence for both conditions (Fig. 4). During the first 6 h of incubation, the fluorescence of cells incubated with Bet v 1 only increased linearly and was always lower than the fluorescence of cells incubated with  $\text{SiO}_2$  NP bound Bet v 1. However, after 24 h of incubation, cells treated with Bet v 1 alone showed a significantly higher fluorescence than cells treated with  $\text{SiO}_2$  NP-bound Bet v 1 (Fig. 4B). The fluorescence of cells incubated with  $\text{SiO}_2$  NP/Bet v 1 conjugates increased fast, reaching a plateau after 2 h of incubation. Similar results were observed for hAELVi cells incubated under ALI conditions; here the fluorescence was also lower for cells incubated with unbound Bet v 1 for 2 h. Contrary to the results for the submerged exposure after 24 h, the cells incubated with unbound Bet v 1 reached a lower fluorescence than the cells exposed to  $\text{SiO}_2$  NP-bound Bet v 1. To determine whether different substrates display a potential influence on the uptake kinetics, control experiments with hAELVi cells were performed. Control cells were grown on Transwell inserts and were incubated under submerged conditions (Fig. S3†). These experiments yielded similar uptake kinetics to the results obtained with cells grown in 24-well plates (Fig. 4).

### 3.5 Localization of taken up Bet v 1 and $\text{SiO}_2$ NPs

For qualitative analysis of the uptake of free Bet v 1 *vs.*  $\text{SiO}_2$  NP-bound Bet v 1, confocal laser scanning microscopy was used. A higher fluorescence signal was observed from the cells incubated with  $\text{SiO}_2$  NP-bound Bet v 1 than for cells incubated with free Bet v 1 incubated under submerged conditions (Fig. 5A and B). Comparable results were observed for ALI-exposed cells. The samples incubated with NP-bound

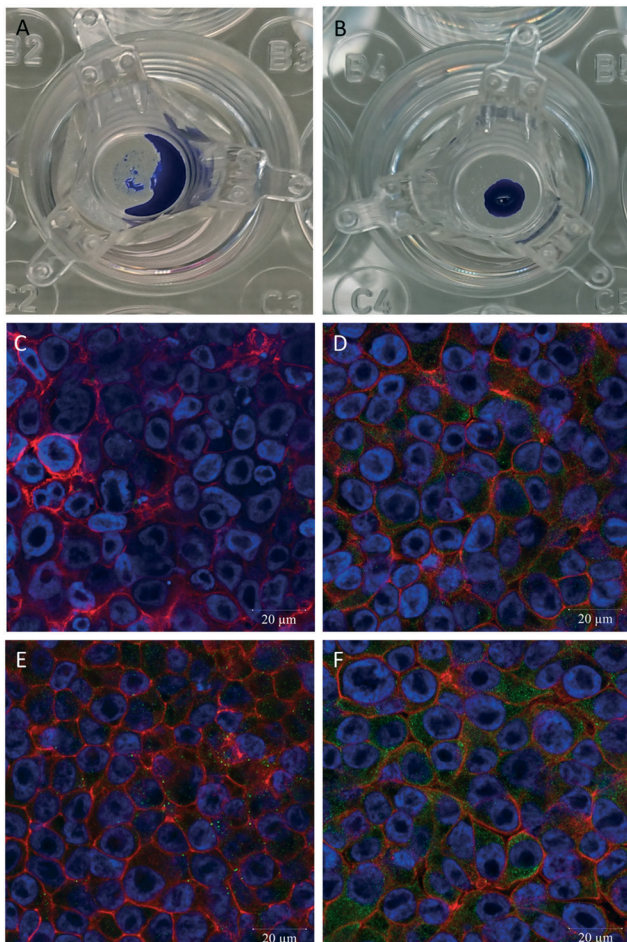


**Fig. 3** Determination of surfactant on hAELVi cells. (A) DMP/O droplet test on cells grown under submerged conditions. (B) DMP/O droplet test on cells grown under ALI conditions. (C-F) Confocal microscopy pictures of cells grown under ALI conditions for determination of surfactant proteins A (D), B (E), and C (F). (C) Second antibody control, actin (red), nuclei (blue), surfactant proteins (green).



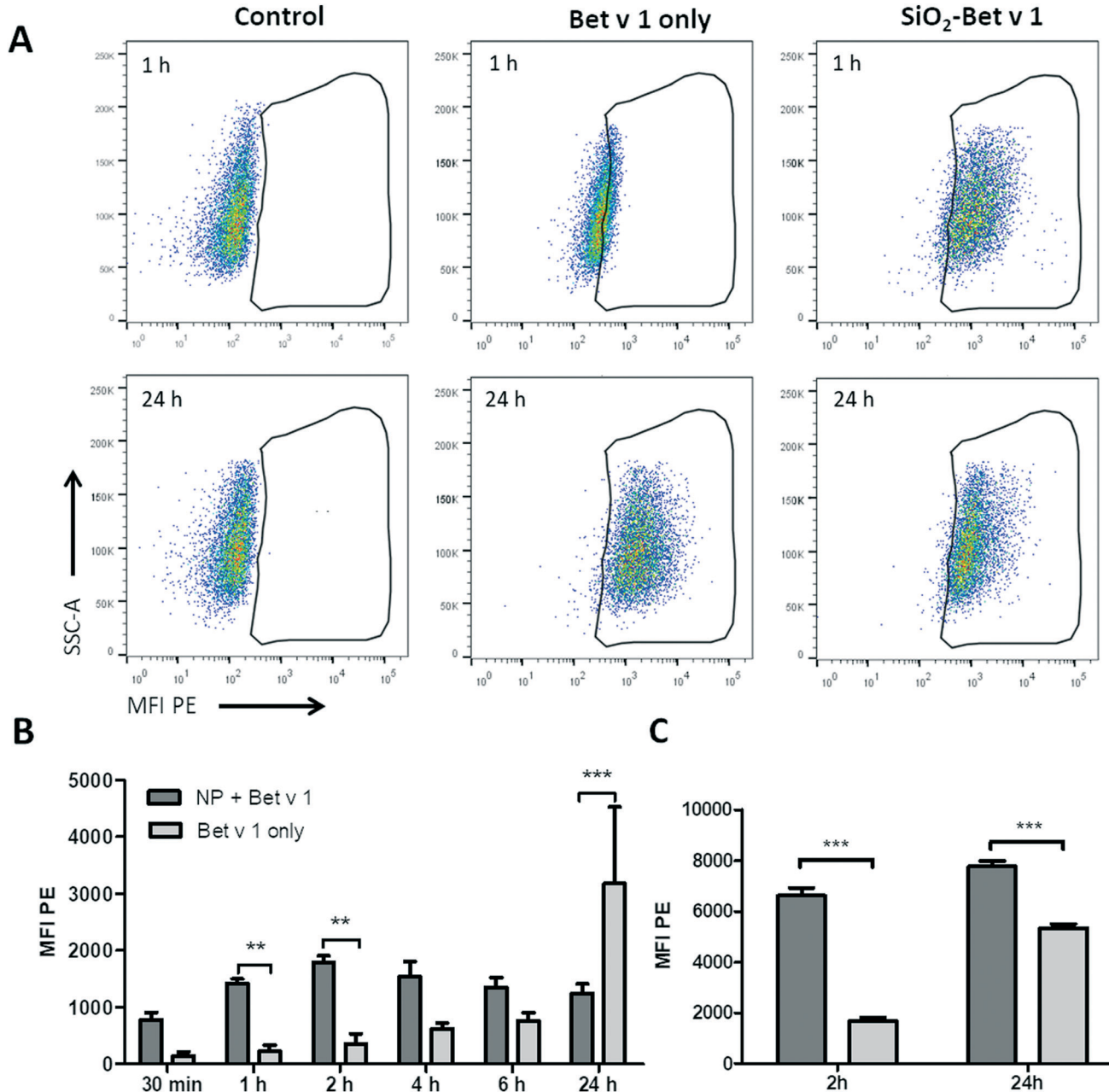


**Fig. 4** Time-resolved uptake of free Bet v 1-pHrodo and  $\text{SiO}_2$  NP-bound Bet v 1-pHrodo measured using flow cytometry. (A) Dot plots of hAELVi cells; control: cells without NPs or Bet v 1, Bet v 1 only: cells incubated with labelled Bet v 1 only,  $\text{SiO}_2$  Bet v 1: cells incubated with NP-bound labelled allergen. (B) Bar chart of mean fluorescence intensity for different time points of cells incubated under submerged conditions. (C) Bar chart of mean fluorescence intensity at 2 h and 24 h of cells incubated under ALI conditions. \*\* $p < 0.01$ , \*\*\* $p < 0.001$ .

Bet v 1 (Fig. 5D) appeared similar to cells incubated under submerged conditions (Fig. 5B), while the free Bet v 1 incubation showed a higher signal under ALI exposure (Fig. 5C) than under submerged exposure (Fig. 5A). The results obtained for incubation times of 2 h correlate with the results shown above by flow cytometry (Fig. 4). z-Stacks revealed that free and NP-bound allergens were found adherent both to the surface and inside the cells, but no quantitative assessment about the distribution inside vs. outside the cell could be made.

### 3.6 Uptake mechanism of unbound vs. $\text{SiO}_2$ NP-associated allergen

For the investigation of the uptake mechanisms of Bet v 1/ $\text{SiO}_2$  NP conjugates and free Bet v 1 by hAELVi cells, cells were pre-incubated with four different inhibitors (Table S2†) under submerged conditions and the uptake was analysed as described above. The viability test revealed that only methyl- $\beta$ -cyclodextrin caused a decrease in cell viability, while the incubation with the other three inhibitors still

allowed a viability of between 80% and 90% for the concentrations used, as summarized in Table S2.<sup>†</sup> When comparing the inhibitors in their functions to reduce the uptake of the conjugates or the protein alone, a significant difference in the median fluorescence intensity could be observed for the conjugates, but not for the free Bet v 1. All three inhibitors used decreased the fluorescence intensity of free Bet v 1 compared to the control. Even though the highest decrease could be observed for CPZ, the difference between the three inhibitors did not reach significance. For the uptake of the allergen–NP conjugates, both CytoD and Noco lowered the median fluorescence intensity significantly compared to CPZ (Fig. 6).

### 3.7 Cytokine expression after incubation

The impact of NP, allergen, and conjugate exposure on hAELVi cells was investigated by determining a panel of pro- and anti-inflammatory cytokines and chemokines. As representatives for a pro-inflammatory response, IL-1 $\alpha$ , IL-1 $\beta$ , IL-8 and TNF- $\alpha$  were determined, while IL-25 and IL-37 were measured for anti-inflammatory profiling. Under submerged conditions, cells incubated with SiO<sub>2</sub> NPs displayed an increased expression of IL-1 $\alpha$ , IL-1 $\beta$ , IL-8, IL-25 and IL-37 (Fig. 7) compared to cells incubated in CCM alone. When Bet v 1–NP conjugates were used for incubation, the expression was further increased compared to the NPs alone. However, statistically significant

differences were found only for the pro-inflammatory cyto-/chemokines IL-1 $\alpha$ , IL-1 $\beta$  and IL-8 when compared to the expression with Bet v 1. For TNF- $\alpha$ , no differences in expression could be observed at all different incubation conditions. The pro-inflammatory markers were significantly upregulated under submerged culture conditions, while under ALI conditions no significant difference in the expression patterns could be observed. Overall, the cyto-/chemokine expression was lower at ALI compared to submerged conditions (Fig. 7).

## 4 Discussion

### 4.1 Characterization of SiO<sub>2</sub> NPs and allergen–NP conjugates under test conditions

In the incubation media used the SiO<sub>2</sub> NPs formed small agglomerates as NTA detected entities of around 200 nm, even though the primary NP size of 80 nm was determined by SEM. For all tested media the particles formed stable colloidal dispersions for up to 45 min as shown by sedimentation analysis (Fig. 1C). At incubation periods of 1 h and longer, the particles start to sediment and the silica content measured in the topmost fraction gradually decreases and reaches almost zero at 24 h. Dosimetry modelling using the ISDD model<sup>45</sup> was conducted to determine the delivered doses for the different exposure time points under submerged culture conditions (Fig. 1D). While at the ALI small microgram amounts of NPs were deposited within a short time period,

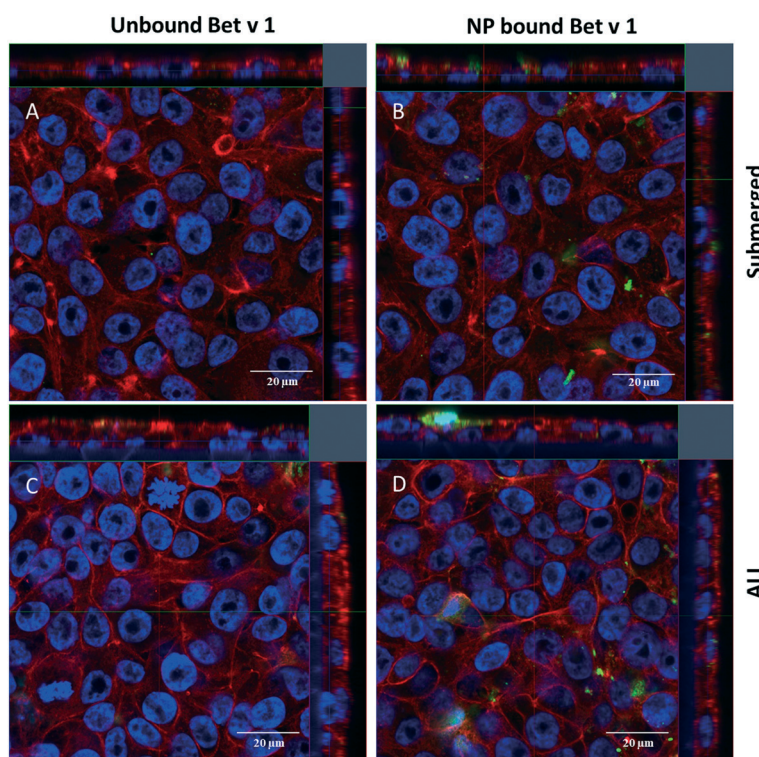


**Fig. 5** Uptake of allergen–NP conjugates or free Bet v 1 by hAELVi cells determined by confocal microscopy. Shown are representative sections from a z-stack of cells incubated for 2 h with free (A) and NP-bound (B) allergen under submerged conditions and free (C) and NP-bound (D) allergen under ALI conditions. Bet v 1 labelled with FITC (green), actin stained with rhodamine (red) and nuclei stained with DAPI (blue).



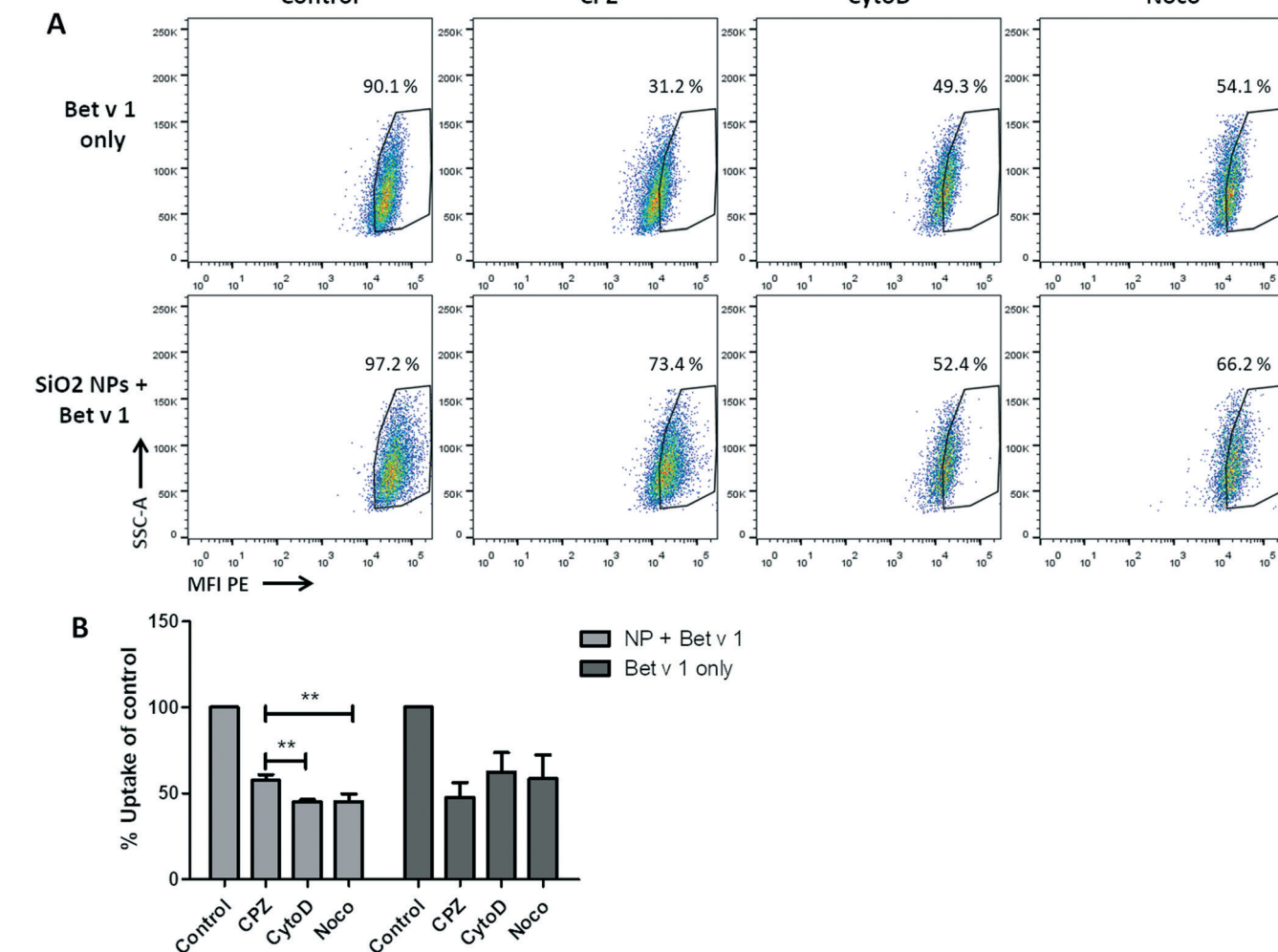


**Fig. 6** NP uptake inhibition in hAELVi cells. (A) Dot blots of unbound Bet v 1-pHrodo (upper), NP-bound Bet v 1-pHrodo (lower), control: without inhibitors, CPZ: chlorpromazine, CytoD: cytochalasin D, Noco: nocodazole. (B) Bar charts of median fluorescence intensity of the different conditions. \*\*p < 0.01.

corresponding amounts of NPs required more than 24 h to be delivered to the cell surface under submerged culture conditions. This delay results in a low comparability of these two exposure systems regarding kinetic assessments combined with a higher expected sensitivity of the ALI towards NP deposition. A future study may investigate the comparability employing other ALI exposure scenarios based on different mechanisms of aerosol delivery onto the cells such as diffusion, impaction or electrostatic deposition.<sup>55</sup>

#### 4.2 Uptake of SiO<sub>2</sub> NPs and SiO<sub>2</sub> NP-allergen conjugates

**4.2.1 Behaviour of hAELVi cells at the air-liquid interface.** The formation of a stable drop of DMP/O on the ALI-cultured hAELVi cells indicates the presence of pulmonary surfactant,<sup>50,56</sup> in contrast to the same cells cultured under submerged conditions, where no droplet was formed. These results were supported by immunostaining against surfactant protein A-C that show the presence of the analysed protein by

a green fluorescence signal for all three antibodies. This is in contrast to previous reports,<sup>34</sup> which applied, however, different experimental conditions. There are so far only 2 publications available providing data on hAELVi cells,<sup>34,35</sup> so experience on this interesting cell line still needs to be gained.

**4.2.2 Time-resolved uptake.** The allergen in the particle bound form was taken up with faster kinetics than that in the unbound allergen. This may, under submerged conditions, be due to faster gravitational sedimentation of the conjugates compared to the free allergen. Contrary to this expectation, the NPs seemed to not sediment for up to 45 minutes in CCM as experimentally evidenced by sedimentation studies. *In vitro* sedimentation dosimetry calculations further elucidated that after 2 h of incubation only approx. 7.1% of the administered NPs and after 24 h approx. 27.0% had deposited onto the cells. In contrast, it takes only 20 min until 50–80% of the material deposits onto the surface of the cells growing at the ALI.<sup>51</sup> We observed maximal MFIs for taken up NP-bound allergen

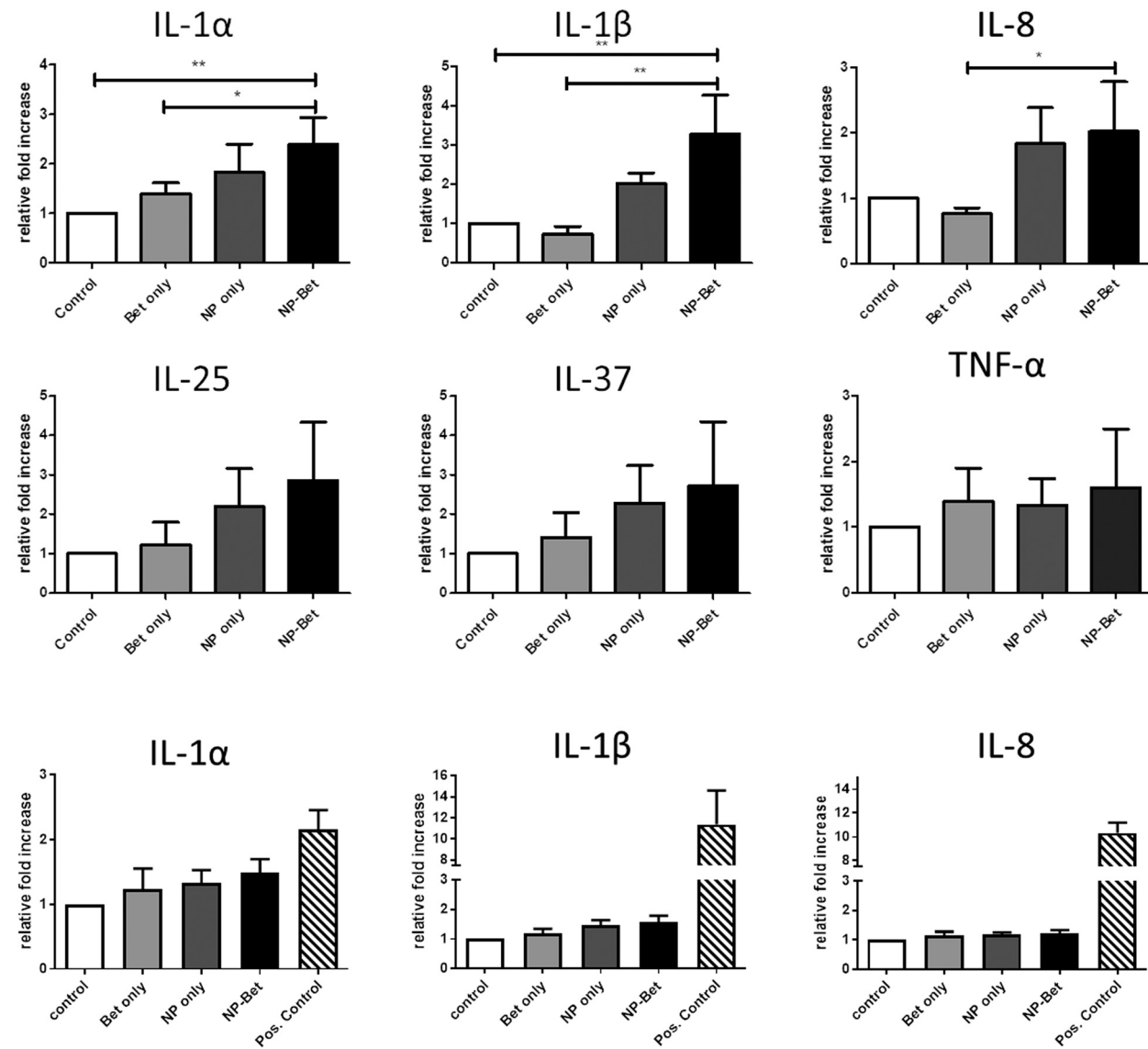


**Fig. 7** Relative expression levels of pro- and anti-inflammatory markers after incubation under submerged and ALI conditions. hAELVi cells were incubated with either  $50 \mu\text{g mL}^{-1}$   $\text{SiO}_2$  NPs,  $5 \mu\text{g mL}^{-1}$  recombinant Bet v 1 or a combination of both. (A) Cytokine expression for incubation under submerged conditions. (B) Cytokine expression for incubation under ALI conditions. Expression levels of markers compared to housekeeping gene GAPDH. \* $p < 0.1$ , \*\* $p < 0.01$ .

already between 1 and 6 h under submerged conditions, while freely diffusing allergen was taken up much more slowly. These results differ from findings published earlier for A549 cells, where the allergen NP conjugates showed a maximum uptake after 24 hours and low uptake for incubation times of one and four hours.<sup>49</sup> At the ALI, however, where similar amounts of unbound and NP-associated allergen have been deposited onto the cells within a short time (approx. 20 min), a similar difference between these two states was observed. This suggests that NP/cell interactions are more relevant here than the culture conditions and that sedimentation might not be the main driving force behind the observed increased uptake. Additionally, the control experiment where hAELVi cells were seeded on Transwell inserts but exposed under

submerged conditions (Fig. S3†) showed similar results to hAELVi cells seeded in 24-well plates. This further emphasizes that NP/cell interactions represent the relevant factor for the modulation in the time kinetics. The difference in uptake of allergen between unbound and NP-associated allergen was higher at 2 h than later. Surprisingly, we observed a significant discrepancy between the maximum MFIs of unbound vs. NP-associated allergen under submerged conditions. A possible explanation may be the pH sensitivity of the pHrodo signal, which depends on the subcellular localization, which could be explained by different uptake mechanisms based on the size and kinetics of uptake. Particle-bound allergen may circumvent locations with low pH due to possible endosomal particle escape,<sup>57</sup> while unbound allergen becomes degraded in the

lysosomes, causing an accumulation of released fluorescent dye in this acidic compartment.

**4.2.3 Uptake mechanism.** The conjugate uptake appears to be mainly facilitated by macropinocytosis since the inhibitors for this mechanism led to the highest degree of uptake inhibition. Even though CPZ also decreased the uptake of the conjugates, both CytoD and Noco led to a significantly higher decrease of the uptake of conjugates compared to CPZ. No statistically significant differences in the uptake of free Bet v 1 could be observed between the used inhibitors but there was a trend suggesting that the free Bet v 1 is mainly mediated by clathrin-dependent uptake. This has to be interpreted with caution, since the inhibitors are not always specific in inhibiting only the intended pathway.<sup>58–60</sup> Keeping all that in mind, the data still strongly suggest different uptake pathways for the free and NP-bound form of allergen. This correlates well with the literature stating that macropinocytosis favours the uptake of bigger entities like NP and conjugates thereof, while the clathrin-mediated mechanism favours smaller entities such as free allergen.<sup>61</sup>

#### 4.3 Immune responses

**4.3.1 Cytokine secretion.** No discernible impact on the viability of subjected cells was observed after NP exposure, but immune markers were affected. An increase in pro-inflammatory cytokine expression was observed under submerged but not under ALI culture conditions. The pro-inflammatory effects of NPs can be an artefact due to contamination with LPS,<sup>62</sup> but our tests showed that endotoxin levels of the NPs at the used concentrations were determined to be  $<0.02 \text{ ng mL}^{-1}$ . LPS concentrations as low as  $0.02 \text{ ng mL}^{-1}$  can activate immune cells such as primary dendritic cells and monocytes,<sup>63</sup> but not epithelial cell lines, as they usually lack the specific LPS receptor component TLR4. The absence of TLR4 receptor on the surface of hAELVi cells was shown by control experiments using flow cytometry (Fig. S2†). In addition, an LPS concentration of  $2 \text{ ng mL}^{-1}$  directly onto the cells did not induce cytokines or chemokines, so we can rule out LPS effects.

When the cells were incubated with NPs, conjugates and unbound allergen under ALI conditions, they were protected from the pro-inflammatory effects observed under submerged culture conditions. Notably, this effect was still detectable even though a much higher amount of material had been deposited within a short time onto the cells. A similar effect of lower sensitivity towards silica NPs has been previously reported for A549 cells at the ALI.<sup>64</sup> The differing susceptibilities of hAELVi cells grown under submerged *vs.* ALI conditions suggest the application of the simpler, more robust, and cost-effective submerged culture system only for studies where immune responses are not relevant, whereas the evaluation of specific immune endpoints requires the more elaborate and sophisticated ALI format, which also closer mimics the human situation. In consequence, the lower susceptibility of cells towards noxious stimuli that was

observed under ALI conditions does not necessarily mean that the hAELVi cells are not a sensitive model. Rather, we assume that under those conditions, as resembling the context of inhalation, a lower observed susceptibility more closely relates to the *in vivo* situation. One possible reason for the difference in effect observed between free and NP-bound Bet v 1 could be the increased uptake. For the 4 hours of incubation, the signal for internalized NP-bound Bet v 1 was twice as high compared to that of the free form. Allergens usually have no effect while outside of cells, unless they bind IgE antibodies bound to high-affinity IgE receptors on the cell membrane. We suggest that the biological effects observed are mediated after internalisation, which can occur *via* different mechanisms for bound and unbound allergen.

## Conclusions

We conducted a methodological mechanistic study using a well-defined allergen-doped particulate system and found that the non-covalent conjugation of allergen to NPs does modify their uptake into epithelial cells while the biological consequences inside the cells varied depending on the cell culture conditions applied. We found that particle association accelerated and intensified the uptake of allergen by human alveolar lung epithelial cells using the currently most relevant cellular model, the hAELVi cells. A two-stage approach was used: (i) submerged culture conditions representing a simpler and more cost-effective setup that allowed a broader range for time-resolved uptake conditions (30 min–24 h) to be tested; it furthermore enabled a mechanistic elucidation and pro-*vs.* anti-inflammatory cyto-/chemokine expression profiling; (ii) this stage was followed by more elaborate and sophisticated exposure conditions of ALI-cultured hAELVi cells employing the Vitrocell-Cloud system. Selected specific readouts were measured, *i.e.* 2 and 24 h for uptake, 4 h for pro-inflammatory cyto-/chemokine profiling. In comparison to the submerged conditions, we observed a lower susceptibility of the cells at the ALI, as no inflammatory cyto-/chemokine responses were induced under these conditions. In summary, hAELVi cells cultured under ALI conditions represent a realistic model for studying the immune effects of NPs and substances associated with them. Nevertheless, potential further interactions, as shown here with environmental allergens, should be considered when assessing the biological impact of nanoparticles.

## Authors' contributions

Experimental work for Fig. 1–7 and Table S2† was performed by RMG, who also prepared the first draft of the manuscript. MS, AF and NHü prepared SiO<sub>2</sub> NPs and operated the SEM. AC contributed to the experimental work for Fig. 4. TS operated the CLSM. SH and NHo performed calculations of nanoparticle settling under culturing conditions (Fig. 1). MH and MG conceived the study. ACG, MH, MG and AD supervised the work. ACG and AD provided infrastructure



and funding relevant for this study. All authors were involved in reviewing and editing the manuscript.

## Conflicts of interest

There are no conflicts to declare.

## Acknowledgements

This work was funded by the international PhD program “Immunity in Cancer and Allergy” of the Austrian Science Fund (FWF, grant no. W01213) and by the Allergy Cancer Bio-Nano Research Centre of the University of Salzburg. The contributions of AC, ACG and TS were supported by the Fonds National de la Recherche (FNR) funded VitralizeMe project (PoC18/12559604).

## References

- 1 T. A. Platts-Mills, The allergy epidemics: 1870-2010, *J. Allergy Clin. Immunol.*, 2015, **136**, 3–13.
- 2 S. F. Thomsen, Epidemiology and natural history of atopic diseases, *Eur. Clin. Respir. J.*, 2015, **2**, 24642.
- 3 E. TEAoAaCI, *Advocacy Manifesto - Tackling the Allergy Crisis in Europe - Concerted Policy Action Needed*, 2015.
- 4 C. A. Akdis and I. Agache, *Global atlas of allergy*, European Academy of Allergy and Clinical Immunology, 2014.
- 5 S. Lee, IgE-mediated food allergies in children: prevalence, triggers, and management, *Korean J. Pediatr.*, 2017, **60**, 99.
- 6 A. L. Lopata and M. F. Jeebhay, Airborne seafood allergens as a cause of occupational allergy and asthma, *Curr. Allergy Asthma Rep.*, 2013, **13**, 288–297.
- 7 G. Brozek, J. Lawson, D. Szumilas and J. Zejda, Increasing prevalence of asthma, respiratory symptoms, and allergic diseases: Four repeated surveys from 1993–2014, *Respir. Med.*, 2015, **109**, 982–990.
- 8 J. N. Larsen, L. Broge and H. Jacobi, Allergy immunotherapy: the future of allergy treatment, *Drug Discovery Today*, 2016, **21**, 26–37.
- 9 R. Pawankar, G. Canonica, S. Holgate and R. Lockey, Executive Summary, in *World Allergy Organization (WAO) White Book on Allergy*, 2011, [https://www.worldallergy.org/UserFiles/file/WAO-White-Book-on-Allergy\\_web.pdf](https://www.worldallergy.org/UserFiles/file/WAO-White-Book-on-Allergy_web.pdf).
- 10 C. W. Schmidt, Pollen Overload: Seasonal Allergies in a Changing Climate, *Environ. Health Perspect.*, 2016, **124**, A70–A75.
- 11 F. Sedghy, A.-R. Varasteh, M. Sankian and M. Moghadam, Interaction between air pollutants and pollen grains: the role on the rising trend in allergy, *Rep. Biochem. Mol. Biol.*, 2018, **6**, 219.
- 12 M. Smith, S. Jäger, U. Berger, B. Šikoparija, M. Hallsdóttir, I. Sauliene, K. C. Bergmann, C. Pashley, L. De Weger and B. Majkowska-Wojciechowska, Geographic and temporal variations in pollen exposure across Europe, *Allergy*, 2014, **69**, 913–923.
- 13 DaNa 2.0 Information about nanomaterials and their safety assessment, <https://www.nanopartikel.info/en/faq/2251> where-can-i-find-current-production-figures-for-nanomaterials, (accessed 16.05., 2019).
- 14 European-Commission, Types and uses of nanomaterials, including safety aspects, Accompanying the Communication from the Commission to the European Parliament, the Council and the European Economic and Social Committee on the Second Regulatory Review on Nanomaterials, 2012, <https://op.europa.eu/en/publication-detail/-/publication/be32dfc7-1499-4328-b54f-a9f024805f59/language-en>.
- 15 F. Piccinno, F. Gottschalk, S. Seeger and B. Nowack, Industrial production quantities and uses of ten engineered nanomaterials in Europe and the world, *J. Nanopart. Res.*, 2012, **14**, 1109.
- 16 D. Napierska, L. C. Thomassen, D. Lison, J. A. Martens and P. H. Hoet, The nanosilica hazard: another variable entity, *Part. Fibre Toxicol.*, 2010, **7**, 39.
- 17 L. R. Khot, S. Sankaran, J. M. Maja, R. Ehsani and E. W. Schuster, Applications of nanomaterials in agricultural production and crop protection: a review, *Crop Prot.*, 2012, **35**, 64–70.
- 18 M. R. Kasai, Nanosized particles of silica and its derivatives for applications in various branches of food and nutrition sectors, *J. Nanotechnol.*, 2015, **2015**, 852394, DOI: 10.1155/2015/852394.
- 19 A. Brinch, S. Hansen, N. Hartmann and A. Baun, EU regulation of nanobiocides: challenges in implementing the biocidal product regulation (BPR), *Nanomaterials*, 2016, **6**, 33.
- 20 C. Liljenström, D. Lazarevic and G. Finnveden, Silicon-based nanomaterials in a life-cycle perspective, including a case study on self-cleaning coatings, *PhD thesis*, KTH - Royal Institute of Technology, 2013, <https://www.diva-portal.org/smash/get/diva2:665233/FULLTEXT02.pdf>.
- 21 AZoM.com Limited, *AZOnano*, <https://www.azonano.com/article.aspx?ArticleID=3398>, (accessed 17.05., 2019).
- 22 V. Mamaeva, C. Sahlgren and M. Lindén, Mesoporous silica nanoparticles in medicine—Recent advances, *Adv. Drug Delivery Rev.*, 2013, **65**, 689–702.
- 23 S. Jafari, H. Derakhshankhah, L. Alaei, A. Fattahi, B. S. Varnamkhasti and A. A. Saboury, Mesoporous silica nanoparticles for therapeutic/diagnostic applications, *Biomed. Pharmacother.*, 2019, **109**, 1100–1111.
- 24 C. C. Leung, I. T. S. Yu and W. Chen, Silicosis, *Lancet*, 2012, **379**, 2008–2018.
- 25 M. Ahamed, Silica nanoparticles-induced cytotoxicity, oxidative stress and apoptosis in cultured A431 and A549 cells, *Hum. Exp. Toxicol.*, 2013, **32**, 186–195.
- 26 E. Maser, M. Schulz, U. G. Sauer, M. Wiemann, L. Ma-Hock, W. Wohlleben, A. Hartwig and R. Landsiedel, In vitro and in vivo genotoxicity investigations of differently sized amorphous SiO<sub>2</sub> nanomaterials, *Mutat. Res., Genet. Toxicol. Environ. Mutagen.*, 2015, **794**, 57–74.
- 27 K. Siegmann, L. Scherrer and H. Siegmann, Physical and chemical properties of airborne nanoscale particles and how to measure the impact on human health, *J. Mol. Struct.: THEOCHEM*, 1998, **458**, 191–201.
- 28 R. Dalefield, in *Veterinary Toxicology for Australia and New Zealand*, ed. R. Dalefield, Elsevier, Oxford, 2017, pp. 233–253, DOI: 10.1016/B978-0-12-420227-6.00013-X.



29 C. Ge, J. Tian, Y. Zhao, C. Chen, R. Zhou and Z. Chai, Towards understanding of nanoparticle–protein corona, *Arch. Toxicol.*, 2015, **89**, 519–539.

30 I. Radauer-Preiml, A. Andosch, T. Hawranek, U. Luetz-Meindl, M. Wiederstein and J. Horejs-Hoeck, Nanoparticle-allergen interactions mediate human allergic responses: protein corona characterization and cellular responses, *Part. Fibre Toxicol.*, 2016, **13**, 3.

31 J. D. Crapo, B. E. Barry, P. Gehr, M. Bachofen and E. R. Weibel, Cell number and cell characteristics of the normal human lung, *Am. Rev. Respir. Dis.*, 1982, **126**, 332–337.

32 M. Lieber, G. Todaro, B. Smith, A. Szakal and W. Nelson-Rees, A continuous tumor-cell line from a human lung carcinoma with properties of type II alveolar epithelial cells, *Int. J. Cancer*, 1976, **17**, 62–70.

33 K. A. Foster, C. G. Oster, M. M. Mayer, M. L. Avery and K. L. Audus, Characterization of the A549 cell line as a type II pulmonary epithelial cell model for drug metabolism, *Exp. Cell Res.*, 1998, **243**, 359–366.

34 A. Kuehn, S. Kletting, C. de Souza Carvalho-Wodarz, U. Repnik, G. Griffiths, U. Fischer, E. Meese, H. Huwer, D. Wirth and T. May, Human alveolar epithelial cells expressing tight junctions to model the air-blood barrier, *Altex*, 2016, **33**, 251–260.

35 S. Kletting, S. Barthold, U. Repnik, G. Griffiths, B. Loretz, N. Schneider-Daum, C. de Souza Carvalho-Wodarz and C. M. Lehr, Co-culture of human alveolar epithelial (hAELVi) and macrophage (THP-1) cell lines, *ALTEX*, 2017, **34**, 211–222.

36 G. J. Oostingh, E. Casals, P. Italiani, R. Cognato, R. Stritzinger, J. Ponti, T. Pfaller, Y. Kohl, D. Ooms and F. Favilli, Problems and challenges in the development and validation of human cell-based assays to determine nanoparticle-induced immunomodulatory effects, *Part. Fibre Toxicol.*, 2011, **8**, 8.

37 J. M. Cohen, J. G. Teeguarden and P. Demokritou, An integrated approach for the in vitro dosimetry of engineered nanomaterials, *Part. Fibre Toxicol.*, 2014, **11**, 20.

38 L. C. Stoehr, C. Endes, I. Radauer-Preiml, M. S. P. Boyles, E. Casals, S. Balog, M. Pesch, A. Petri-Fink, B. Rothen-Rutishauser, M. Himly, M. J. D. Clift and A. Duschl, Assessment of a panel of interleukin-8 reporter lung epithelial cell lines to monitor the pro-inflammatory response following zinc oxide nanoparticle exposure under different cell culture conditions, *Part. Fibre Toxicol.*, 2015, **12**, 29.

39 I. Radauer-Preiml, A. Andosch, T. Hawranek, U. Luetz-Meindl, M. Wiederstein, J. Horejs-Hoeck, M. Himly, M. Boyles and A. Duschl, Nanoparticle-allergen interactions mediate human allergic responses: protein corona characterization and cellular responses, *Part. Fibre Toxicol.*, 2016, **13**, 3.

40 E. Zahradník and M. Raulf, Animal allergens and their presence in the environment, *Front. Immunol.*, 2014, **5**, 76.

41 S. De Lucca, R. Sporik, T. J. O'Meara and E. R. Tovey, Mite allergen (Der p 1) is not only carried on mite feces, *J. Allergy Clin. Immunol.*, 1999, **103**, 174–175.

42 G. F. Schäppi, C. Suphioglu, P. E. Taylor and R. B. Knox, Concentrations of the major birch tree allergen Bet v 1 in pollen and respirable fine particles in the atmosphere, *J. Allergy Clin. Immunol.*, 1997, **100**, 656–661.

43 A. Feinle, F. Leichtfried, S. Straßer and N. Hüsing, Carboxylic acid-functionalized porous silica particles by a co-condensation approach, *J. Sol-Gel Sci. Technol.*, 2017, **81**, 138–146.

44 T. Coradin, D. Eglin and J. Livage, The silicomolybdc acid spectrophotometric method and its application to silicate/biopolymer interaction studies, *J. Spectrosc.*, 2004, **18**, 567–576.

45 P. M. Hinderliter, K. R. Minard, G. Orr, W. B. Chrisler, B. D. Thrall, J. G. Pounds and J. G. Teeguarden, ISDD: a computational model of particle sedimentation, diffusion and target cell dosimetry for in vitro toxicity studies, *Part. Fibre Toxicol.*, 2010, **7**, 36.

46 G. DeLoid, J. M. Cohen, T. Darrah, R. Derk, L. Rojanasakul, G. Pyrgiotakis, W. Wohlleben and P. Demokritou, Estimating the effective density of engineered nanomaterials for in vitro dosimetry, *Nat. Commun.*, 2014, **5**, 3514.

47 M. Wallner, M. Himly, A. Neubauer, A. Erler, M. Hauser, C. Asam, S. Mutschlechner, C. Ebner, P. Briza and F. Ferreira, The influence of recombinant production on the immunologic behavior of birch pollen isoallergens, *PLoS One*, 2009, **4**, e8457.

48 N. Zaborsky, M. Brunner, M. Wallner, M. Himly, T. Karl, R. Schwarzenbacher, F. Ferreira and G. Achatz, Antigen aggregation decides the fate of the allergic immune response, *J. Immunol.*, 2010, **184**, 725–735.

49 B. Grotz, M. Geppert, R. Mills-Goodlet, S. Hofer, N. Hofstätter, C. Asam, A. Feinle, K. Kocsis, T. Berger and O. Diwald, Biologic effects of nanoparticle-allergen conjugates: time-resolved uptake using an in vitro lung epithelial co-culture model of A549 and THP-1 cells, *Environ. Sci.: Nano*, 2018, **5**, 2184–2197.

50 S. Schürch, J. Goerke and J. A. Clements, Direct determination of volume-and time-dependence of alveolar surface tension in excised lungs, *Proc. Natl. Acad. Sci. U. S. A.*, 1978, **75**, 3417–3421.

51 I. Fizeşan, S. Cambier, E. Moschini, A. Chary, I. Nelissen, J. Ziebel, J.-N. Audinot, T. Wirtz, M. Kruszewski, A. Pop, B. Kiss, T. Serchi, F. Loghin and A. C. Gutleb, In vitro exposure of a 3D-tetraculture representative for the alveolar barrier at the air-liquid interface to silver particles and nanowires, *Part. Fibre Toxicol.*, 2019, **16**, 14.

52 G. Repetto, A. Del Peso and J. L. Zurita, Neutral red uptake assay for the estimation of cell viability/cytotoxicity, *Nat. Protoc.*, 2008, **3**, 1125.

53 M. S. Boyles, C. Ranninger, R. Reischl, M. Rurik, R. Tessadri, O. Kohlbacher, A. Duschl and C. G. Huber, Copper oxide nanoparticle toxicity profiling using untargeted metabolomics, *Part. Fibre Toxicol.*, 2015, **13**, 49.

54 J. Schindelin, I. Arganda-Carreras, E. Frise, V. Kaynig, M. Longair, T. Pietzsch, S. Preibisch, C. Rueden, S. Saalfeld and B. Schmid, Fiji: an open-source platform for biological-image analysis, *Nat. Methods*, 2012, **9**, 676–682.



55 E. Frijns, S. Verstraelen, L. C. Stoehr, J. Van Laer, A. Jacobs, J. Peters, K. Tirez, M. S. P. Boyles, M. Geppert, P. Madl, I. Nelissen, A. Duschl and M. Himly, A Novel Exposure System Termed NAVETTA for In Vitro Laminar Flow Electrodeposition of Nanoaerosol and Evaluation of Immune Effects in Human Lung Reporter Cells, *Environ. Sci. Technol.*, 2017, **51**, 5259–5269.

56 D. D. Nalayanda, Q. Wang, W. B. Fulton, T.-H. Wang and F. Abdullah, Engineering an artificial alveolar-capillary membrane: a novel continuously perfused model within microchannels, *J. Pediatr. Surg.*, 2010, **45**, 45–51.

57 L. I. Selby, C. M. Cortez-Jugo, G. K. Such and A. P. R. Johnston, Nanoescapology: progress toward understanding the endosomal escape of polymeric nanoparticles, *Wiley Interdiscip. Rev.: Nanomed. Nanobiotechnol.*, 2017, **9**, e1452.

58 D. A. Kuhn, D. Vanhecke, B. Michen, F. Blank, P. Gehr, A. Petri-Fink and B. Rothen-Rutishauser, Different endocytotic uptake mechanisms for nanoparticles in epithelial cells and macrophages, *Beilstein J. Nanotechnol.*, 2014, **5**, 1625.

59 Z. Garaiova, S. P. Strand, N. K. Reitan, S. Lélu, S. Ø. Størset, K. Berg, J. Malmo, O. Folasire, A. Bjørkøy and C. L. Davies, Cellular uptake of DNA-chitosan nanoparticles: The role of clathrin- and caveolae-mediated pathways, *Int. J. Biol. Macromol.*, 2012, **51**, 1043–1051.

60 T.-G. Iversen, T. Skotland and K. Sandvig, Endocytosis and intracellular transport of nanoparticles: Present knowledge and need for future studies, *Nano Today*, 2011, **6**, 176–185.

61 B. Yameen, W. I. Choi, C. Vilos, A. Swami, J. Shi and O. C. Farokhzad, Insight into nanoparticle cellular uptake and intracellular targeting, *J. Controlled Release*, 2014, **190**, 485–499.

62 Y. Li, M. Fujita and D. Boraschi, Endotoxin contamination in nanomaterials leads to the misinterpretation of immunosafety results, *Front. Immunol.*, 2017, **8**, 472.

63 H. Schwarz, M. Schmittner, A. Duschl and J. Horejs-Hoeck, Residual Endotoxin Contaminations in Recombinant Proteins Are Sufficient to Activate Human CD1c<sup>+</sup> Dendritic Cells, *PLoS One*, 2014, **9**, e113840.

64 A. Panas, A. Comouth, H. Saathoff, T. Leisner, M. Al-Rawi, M. Simon, G. Seemann, O. Dössel, S. Mülhopt and H.-R. Paur, Silica nanoparticles are less toxic to human lung cells when deposited at the air–liquid interface compared to conventional submerged exposure, *Beilstein J. Nanotechnol.*, 2014, **5**, 1590–1602.

